Giant Moses Effect in Ferrofluids in Axial-Symmetric Magnetic and Electric Fields

S. Bednarek*

Department of Physics and Applied Informatics, University of Lodz, 90-236 Łódź, 149/153 Pomorska Str., Poland

Received: 14.05.2025 & Accepted: 28.07.2025

Doi: 10.12693/APhysPolA.148.57 *e-mail: stanislaw.bednarek@uni.lodz.pl

The article provides a generalized definition of the Moses effect, which is described as a change in the shape of a liquid's free surface due to interaction with different force fields. It provides a review of previous results and examples of new opportunities to study this effect. One example was realized using ferrofluid. As a result, the fluid level changed by 10^4–10^5, which is greater than the change in diamagnetic or paramagnetic liquids, and the changes agreed well with the predictions. The article proposes a scheme for organizing future studies of the Moses effect, which can also be easily used as attractive demonstration experiments.

topics: Moses effect, magnetic field, symmetry, ferrofluid

1. Introduction

According to previous publications, the Moses effect in physics is the name of the phenomenon that consists in changing the shape of the free surface of a liquid as a result of its interaction with an inhomogeneous magnetic field [1, 2]. If the liquid is diamagnetic, i.e., its relative magnetic permeability meets the condition $\mu_r < 1$, it is pushed out of the area filled by a stronger magnetic field [3]. This causes the liquid level in the area of the stronger magnetic field to decrease and the free surface of the liquid to assume a concave shape. This variant of the phenomenon is called the simple Moses effect (Fig. 1a; all figures in the article were made by the author). For a paramagnetic liquid, the condition $\mu_r > 1$ occurs, and the liquid is pulled into the region of a stronger magnetic field. This results in the free surface of the liquid having a convex shape; this variant of the phenomenon is called the inverse Moses effect (Fig. 1b).

The described phenomenon is called the Moses effect due to its analogy to the event described in the Old Testament in the "Book of Exodus". According to the description, Moses raised his staff above the surface of the Red Sea. The water then spread sideways and formed a deep gorge to the bottom, through which the Israelites safely escaped from the Egyptian soldiers.

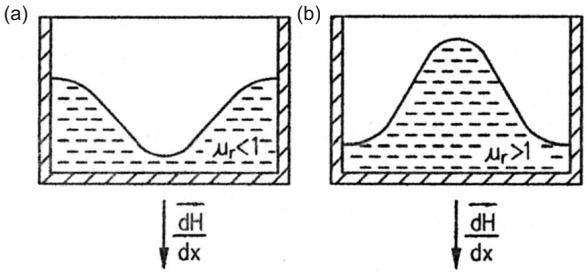

Fig. 1. Two types of the Moses effect in a magnetic field: (a) simple, (b) reverse; H — magnetic field intensity, μ_r — relative magnetic permeability of the liquid, $\mathrm{d}H/\mathrm{d}x$ — magnetic field gradient directed vertically.

2. Overview of previous research

The characteristics of the results of research on the Moses effect to date can be presented in the following points.

(i) The research is concerned with changes in the height of the level of a liquid and the shape of its surface caused by a magnetic field.

(ii) Mainly diamagnetic liquids have been used for these studies.

(iii) Some studies examine the applications of the Moses effect, including determining the magnetic susceptibility of liquids and in innovative technologies.

A representative example of a set of publications containing the results presented in these sections is a dissertation authored by David Shulman [4]. In this work, the results of theoretical and experimental studies on the surface shape of liquids such as water, glycerol, and ethanol, placed in a magnetic field, are reported. The magnetic field producing these changes had cylindrical symmetry and was produced by a permanent magnet placed over the liquid [5]. Because of the small changes in the height of the level of the liquids under study, it was necessary to use Michelson and Mach–Zehnder interferometers for measurements [6, 7].

The results of the conducted measurements were used to determine the magnetic susceptibility of these fluids [8, 9]. Another publication [10] also describes the application of the Moses effect in innovative technologies, including the production of semiconductor circuits and contact formation. The influence of the Moses effect is also considered in studies of anomalous diffusion occurring at the boundary of two liquids and changes in the shape of the surface forming the boundary of these liquids [11, 12]. Other authors have evaluated the Moses effect in the behavior of a diamagnetic liquid in a magnetic field with a large gradient [13], the change in the immersion of a floating body with diamagnetic properties, and also used this effect to determine the magnetic susceptibility of liquids [1, 14, 15]. The importance of the Moses effect in particle trapping and surface rippling of liquids in a magnetic field, modulated on a microscopic scale, has also been demonstrated [16].

The most general mathematical description of the Moses effect given in the literature is an approximation and involves considering two forces [17]. The first force is the result of the interaction of the fluid with the magnetic field, and the second with the gravitational field. The magnetic field under consideration has cylindrical symmetry and most often is generated by permanent magnets in the shape of a cylinder or ring or by cylindrical coils [18, 19]. At equilibrium, the free surface of the fluid at any point aligns perpendicular to the resultant of the two forces. If the additional assumption is made that the interaction force with the magnetic field has a horizontal and radial direction, then according to this description, the change in liquid level height $h(r)$ due to the Moses effect is expressed by the formula

$$h(r) = \frac{\chi B^2(r)}{2\mu_0 \rho g}, \tag{1}$$

where B is the field induction, χ and ρ are the magnetic susceptibility and density of the liquid, respectively, g is the acceleration of the Earth, and $\mu_0 \approx 4\pi \times 10^{-7}$ (V s)/(A m) and denotes the magnetic permeability of a vacuum. (The exact value of μ_0 is determined from the fine structure constant α). Such a formula (1) is given in publications containing general information about the Moses effect and in works that have an educational character [20, 21].

3. New research opportunities

The review of prior results presented in the previous paragraph does not exhaust all the ways to produce the Moses effect and conduct research. Suggestions for new ways and research problems include:

- Using a different type of field and forces, e.g.,
  - electric;
  - gravitational;
  - centrifugal forces;
  - gas pressure;
  - radiation pressure;
  - magnetic, generated by a current flowing in a liquid;
  - magnetic or electric with spatial non-axial distribution;
  - time-dependent.
- The use of another type of medium, e.g.,
  - ferrofluid with dielectric properties,
  - electrically conductive ferrofluid,
  - electrofluid,
  - liquid with permeability dependent on field intensity,
  - powdered materials.
- Formulation of new research problems, e.g.,
  - the generalization of the equation of the liquid surface for any spatial distribution of the field,
  - the equation of the liquid surface for a time-dependent field (for description of the so-named dynamical Moses effect).

Some of these issues are discussed in the upcoming sections of this article.

The understanding of the Moses effect in the publications cited earlier — as a change in the shape of the free surface due to the action of an inhomogeneous magnetic field on this liquid — needs to be extended. For methodological and didactic reasons, it makes sense to generalize the definition of this effect and express it as follows. Namely, the Moses effect is a change in the shape of the free surface of a liquid or powdered medium caused by the interaction of these media with any constant or time-dependent force field (definition formulated by the author). Note, however, that during this interaction, the free surface of the liquid remains perpendicular to the resultant of all acting forces. In other words,

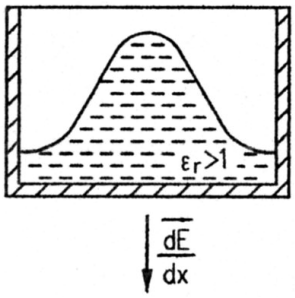

Fig. 2. Moses effect in the electric field; E — electric field intensity, ε_r — relative permeability of the liquid, $\mathrm{d}E/\mathrm{d}x$ — electric field gradient directed vertically.

the free surface remains perpendicular to the gradient of the effective potentials of these forces. The given condition must be satisfied in the equilibrium state of the liquid at each point of its free surface. The purpose of introducing a generalized definition is to systematize the results and possible research directions of the Moses effect.

It is known that the molecules of a liquid placed in an electric field interact with this field and undergo dielectric polarization [22]. If the electric field is inhomogeneous, the Moses effect will also appear on the surface of the liquid. Since the relative electric permeability of liquids satisfies the condition $\varepsilon_r > 1$, the electric field will pull the liquid into the area of the field with higher intensity [3]. Therefore, only the inverse Moses effect appears in the electric field (Fig. 2).

The large-scale Moses effect is also caused by the inhomogeneous gravitational field. The values of gravitational acceleration g at the Earth's surface are in the range of 9.79–9.83 m/s^2. The average depth of the oceans is 3.73 km [23, 24]. Using these values and comparing hydrostatic pressures, it is possible to estimate the change in the height of the ocean level on a global scale, yielding a result of 14.9 m. In practice, this change in height is difficult to measure accurately due to disturbances caused by, among other things, water surges. However, such changes need to be accounted for in accurate geodetic measurements and the creation of increasingly better models of the Earth's surface. It is known that the surface of the oceans and seas at any point is perpendicular to the vertical direction determined by the Earth's effective acceleration. This acceleration is the resultant of local gravitational acceleration and centrifugal force acceleration. As a result, the Earth's surface has a shape similar to a tri-axial ellipsoid and is called a geoid. Increasing the accuracy of vertical direction and geoid determination is of fundamental importance for modern technologies, such as in building construction. As the liquid is pulled into the area of a stronger gravitational field, only the reverse Moses effect can occur in this field.

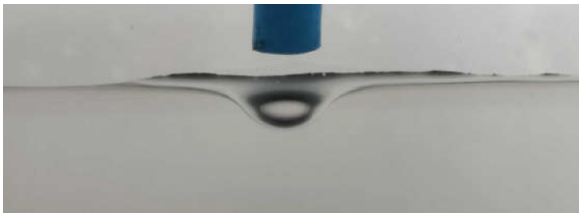

Fig. 3. Moses effect produced by a stream of air flowing out from the tube to the surface of the water. (Photo made by the author).

The Moses effect can be easily produced under laboratory conditions using a jet of gas, flowing out of a nozzle with a diameter of a few millimeters and directed perpendicularly or obliquely to the surface of the liquid. In this case, the free surface of the liquid under the area of gas pressure is lowered. This results in the formation of a cavity, i.e., the appearance of a positive Moses effect. In this description, it was assumed that the jet hits the water surface perpendicularly at a speed of 5 m/s, and the two pressures were compared. As a result, a height change of 1.5 mm was calculated. In order to estimate the value, two pressures should be compared. The first is the hydrostatic pressure caused by this change in height. The second is the dynamic pressure of the air jet described by Bernoulli's equation. An example of the Moses effect produced in this way is shown in Fig. 3.

The pressure needed to cause the Moses effect can also be exerted by high-intensity electromagnetic radiation incident on the surface of a liquid. The pressure of electromagnetic radiation, p, is expressed by

$$p = \frac{P}{cS}(1+r), \tag{2}$$

in which P is the radiation power, S — surface area, c — speed of light in vacuum ($c = 3\times10^8$ m/s), and r — reflection coefficient [25]. One source of high-power electromagnetic radiation is a pulsed magnetron, which emits microwaves with a power of up to 10 MW in the order of a few μs [26]. Let us assume that such a pulse, when focused, has a cross-sectional area of 10 cm^2 and undergoes absorption by water ($r = 0$). In addition, let the exerted radiation pressure be balanced by the hydrostatic pressure of the water. Then, from (2), the change in water level height of 3.3 mm is obtained. This value is obtained by comparing the hydrostatic pressure and radiation pressure from (2) and elementary calculations. Due to the short pulse time, a high-speed camera will be required to record the image, but the Moses effect in this case may prove interesting. It is also worth mentioning that much higher powers of electromagnetic radiation on the order of 10^{18} W are achieved using ultrashort laser pulses [27, 28].

Previous studies of the Moses effect have used diamagnetic liquids. This caused changes in the height of the liquid level on the order of micrometers and difficulties in observation. A few decades ago, stable suspensions of particles with much stronger magnetic properties in liquids were produced and are known as magnetofluids or ferrofluids [29, 30]. Using these suspensions to study the Moses effect will make it possible to obtain directly observable changes in the height of liquid levels. Similar types of liquids are stable suspensions of micro- or nanoparticles of solids in a liquid, called electrofluids or electroreological liquids [31]. These liquids show a strong interaction with the electric field, and therefore, the observation of the Moses effect in these media is easier than in other liquids placed in an electric field. Both types of suspensions also exhibit rheological properties under magnetic or electric fields. Therefore, the Moses effect may exhibit new and interesting features in these suspensions, for example, hysteresis or so-called "shape memory." According to a generalized definition, an example of the Moses effect is also the parabolic depression of the free surface of a liquid, observed in a rotating vessel. In addition, in recent years, suspensions of magnetic particles that conduct electricity have been produced [32]. For this purpose, molten salts were used. When current flows through such suspensions, a magnetic field is also generated inside these suspensions. This results in electrodynamic forces acting on the conductive suspension, which can cause changes in the shape of its surface. This provides a new way of producing the Moses effect that has not been studied before.

In powdered materials placed in a magnetic or electric field, the Moses effect can also occur. If the grains of these powders have ferromagnetic properties, the Moses effect will be easy to observe in a field of low intensity. Of course, the effect of a magnetic field on ferromagnetic filings has been known since the early days of the science of magnetism and used to image the field. Much more interesting is the demonstration of the Moses effect using dia- or paramagnetic powder. To achieve this for a small field strength, the vessel containing the powder must be set into vibration. Similar effects can be achieved in an electric field using grains of ferroelectric materials, such as barium titanate $BaTiO_3$. Interestingly, in the historical description of the Moses effect in Genesis, the free surface of water must have formed the walls of a long corridor, while in the cited studies, this surface took the shape of a cylindrical symmetric rise or depression. This historical variant of the Moses effect can be reproduced under laboratory conditions. To do this, one must use either a perpendicular-shaped magnet or a rectilinear conductor with current, placed horizontally under the bottom of a liquid vessel, to create a magnetic field. If the Moses effect is to be observed in an electric field, a conductor placed in the same way should be charged using a high-voltage source.

4. Advantages of choosing ferrofluid

As mentioned earlier, ferrofluids are stable suspensions of magnetic material particles in a liquid such as oil, or in water, called a dispersion liquid [33, 34]. Since the particle size is 10^{-9}–10^{-8} m, these particles are called nanoparticles. The materials used to make nanoparticles are usually magnetite or hematite. Although the density of the nanoparticle material is greater than that of the dispersion liquid, the nanoparticles do not sink to the bottom of the vessel under the action of their weight. This is because the nanoparticles perform Brownian motions and, as a result, fill the entire volume of the dispersion liquid. Unfortunately, the nanoparticles tend to join together and form agglomerates of larger sizes, which sink to the bottom of the vessel. To prevent this unfavorable phenomenon, the surfaces of the nanoparticles are coated with a layer of surfactant, such as oleic acid, which prevents the particles from connecting.

The total volume of nanoparticles suspended in the dispersion liquid is usually within 5–15% of the volume of ferrofluid. The volume of surfactant is about 10%. The remaining volume of the ferrofluid is filled by the dispersion liquid. Thus, ferrofluids not placed in a magnetic field have properties similar to ordinary liquids. Most particles of the given sizes contain only one magnetic domain. Therefore, no hysteresis occurs during magnetization of ferrofluids, although their magnetization curve may be nonlinear [35]. The relative magnetic permeability of ferrofluids μ_r is much higher than that of paramagnetic substances, and usually has a value of several to a dozen. It was also possible to produce ferrofluids with $\mu_r = 120$–150 at 200 K and a record value of $\mu_r \approx 200$ at liquid nitrogen temperature [33]. As a result, ferrofluids exhibit readily observable interaction with a magnetic field, even of low intensity. This is one of the important features that distinguish ferrofluids from dia- and paramagnetic liquids.

The magnetic field causes an increase in the viscosity of ferrofluids, which causes them to acquire the properties of rheological liquids. This makes it possible, among other things, to direct the movement of ferrofluids and obtain the non-zero modulus of rigidity characteristic of solids. If the intensity of the magnetic field is higher than the critical one, instabilities appear in the ferrofluids [36]. Then, inside the ferrofluid, the particles merge into long fibers and group into columns. This manifests itself by the formation of characteristic deformations on the free surface of the ferrofluid, similar to spikes or needles [37]. Due to the unique combination of liquid, magnetic, and rheological properties and the easy control of these properties using a magnetic field, ferrofluids have found numerous applications [38, 39]. The range of these applications

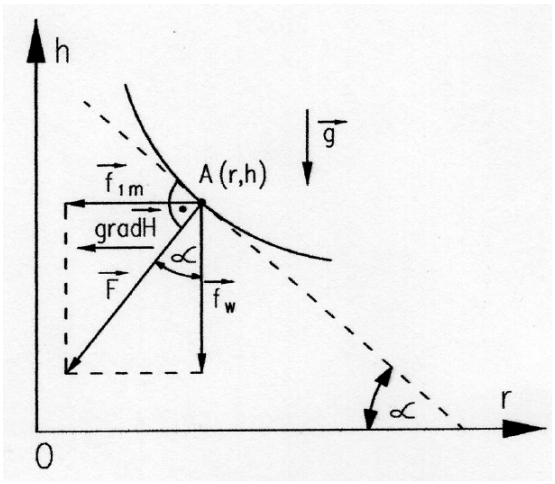

Fig. 4. Forces acting on a volume element of a liquid placed at a point $A(r,h)$ in an cylindrical symmetric magnetic field with a horizontally directed magnetic field gradient: f_{1m} — horizontal component of the magnetic force acting on a volume unit of the liquid, f_w — weight of the volume unit of the liquid, g — acceleration due to Earth's gravity, α — angle of inclination of the tangent to the free surface of the liquid.

is very diverse and includes, among others, control of drug dosage during cancer chemotherapy, vibration dampers, sensors, filters, and magnetic field-controlled transducers [40–42]. The Moses effect is an interesting phenomenon not only for cognitive reasons, but also because of its applications in advanced technologies, including enabling and improving the performance of speakers, electronic circuits, and even creating innovative artistic arrangements [43].

The previously cited articles concern the Moses effect in diamagnetic liquids and are limited to cases in which the spatial distribution of the magnetic field has cylindrical symmetry and the source of this field is located under the bottom of the liquid vessel or above the surface of the liquid [4]. The purpose of the considerations carried out in the following sections of this article is to analyze (1), known from the literature, and to generalize this formula to similar spatial distributions of the field produced by other sources. To verify the obtained calculation results, ferrofluid, i.e., a liquid in which the Moses effect has not yet been studied will be used.

5. Basic formula for a magnetic field with cylindrical symmetry

The Moses effect is described by giving a formula for the height of the liquid level $h(r)$ at a point located at a distance r from the field's axis of symmetry [4, 5]. Using the magnetic field intensity H and the relative magnetic permeability μ_r, (1) can be written in the form of

$$h(r) = \frac{\mu_0(\mu_r - 1)\, H^2(r)}{2\rho\, g}. \tag{3}$$

Formula (3) was derived under the following assumptions [4]. The first assumption is that the spatial distribution of the magnetic field has the so-called cylindrical symmetry, whose axis of symmetry is directed vertically. The symbol r denotes the distance from the axis of symmetry measured in the radial direction. The second assumption is that the magnetic force acts on the liquid only in the radial direction. The direction of the magnetic force is determined by the gradient of the field. Therefore, the gradient must have only one radially directed component, whose value depends on the variable r.

In order to derive (3), the formula known from electrodynamics for the force $\boldsymbol{f}_m$ acting on a unit volume of a material placed in a magnetic field [25] is used, i.e.,

$$\boldsymbol{f}_m = \Big[\mu_0(\mu_r - 1)\boldsymbol{H} \cdot \nabla\Big]\boldsymbol{H}. \tag{4}$$

Formula (4) is valid for a homogeneous material with constant magnetic permeability μ_r. Reducing (4) for one direction determined by radius r and using the symbols given in Fig. 4, it is possible to write a formula for the magnetic force f_{1m} that acts on a unit volume of liquid

$$f_{1m} = \mu_0(\mu_r - 1)H\,\frac{\mathrm{d}H}{\mathrm{d}r}. \tag{5}$$

In addition, the weight of the liquid f_w can be expressed by the formula

$$f_w = \rho\, g, \tag{6}$$

and acts on a unit volume of the liquid.

If the liquid is in equilibrium, the resultant of the forces f_{1m}, i.e., f_w, must be perpendicular to the free surface of the liquid. In the axial section, the free surface of the liquid becomes a line, the shape of which is described by the function $h(r)$. According to the designations given in Fig. 4 and the given equilibrium condition of the liquid, the equation

$$t\,g\,\alpha = \frac{\mathrm{d}h}{\mathrm{d}r} = \frac{f_{1m}}{f_w} \tag{7}$$

can be written.

After substituting (5) and (6) into (7), the following differential equation is obtained

$$\frac{\mathrm{d}h}{\mathrm{d}r} = \frac{\mu_0(\mu_r - 1)\, H\, \frac{\mathrm{d}H}{\mathrm{d}r}}{\rho g}. \tag{8}$$

Making the simplifying assumption that the relative magnetic permeability does not depend on the intensity of the applied magnetic field ($\mu_r = \mathrm{const}$), (8) can be solved by direct integration of both sides. As a result, one obtains

$$h(r) = \frac{\mu_0(\mu_r - 1)\, H^2(r)}{2\rho g}. \tag{9}$$

TABLE I

Comparison of changes in the height of the liquid level $h(r)$ caused by the Moses effect in magnetic and electric fields.

Magnetic field intensity $H(r) = 8 \times 10^4$ A/m ($B(r) = 0.15$ T)			
Properties of the liquid			$h(r)$ [mm]
Type	ρ [kg/m^3]	$(\mu_r - 1)$	
diamagnetic	10^3	-10^{-7}	0.0004
paramagnetic	10^3	10^{-6}	0.004
ferrofluid	1.1×10^3	2	36
Electric field intensity $E(r) = 8 \times 10^4$ V/m			
Properties of the liquid			$h(r)$ [mm]
Type	ρ [kg/m^3]	$(\varepsilon_r - 1)$	
non-polar	10^3	2	0.007
polar	10^3	20	0.066

Now, (9) is identical to (3). Keeping the assumptions made, the given derivation can be repeated for an electric field of intensity E. The result is

$$h(r) = \frac{\varepsilon_0(\varepsilon_r - 1)\, E^2(r)}{2\rho g}, \tag{10}$$

in which $\varepsilon_0 = 8.85 \times 10^{-12}$ F/m and denotes the electrical permeability of the vacuum.

Equation (8) can also be written in the following form

$$\rho g \, \mathrm{d}h = \mu_0(\mu_r - 1) H \, \mathrm{d}H. \tag{11}$$

The left side of (11) denotes the elementary change in the hydrostatic pressure of the liquid, dp, caused by the action of an inhomogeneous magnetic field. This pressure change causes a change in the liquid level by dh in the direction of the field gradient. Integrating (11) also gives (9). This means that (9) can also be used to calculate the change in liquid level caused by a magnetic field whose gradient is directed along the vertical axis. One example of such a situation is a liquid in a vertical capillary placed in a magnetic field with a gradient directed along the axis of the capillary. A magnetic field with this gradient is produced, among other things, by an infinitely long, rectilinear, and horizontal conductor with a current whose axis intersects with the axis of the capillary. Such an electric field gradient yields, for example, a pointed or spherical symmetric charge if its center is on the axis of the capillary.

Note that (9) and (10) allow calculating and comparing the values of $h(r)$, caused by the Moses effect. For this purpose, the average values of the parameters μ_r, ε_r, and ρ for the types of liquids analyzed in the introduction of publication [4] were assumed from tables. Also assumed were the values of H and E produced using readily available neodymium magnets or power supplies found in average-equipped laboratories. The results of the calculations are given in Table I.

The obtained results allow the following conclusion. For diamagnetic and paramagnetic liquids, the liquid level heights $h(r)$ caused by the Moses effect in the magnetic fields considered are of the order of 1 μm or less. Such small values make the observations and measurements of $h(r)$ difficult and require special methods, such as the use of interferometers [4, 44]. The situation is similar in the case of the Moses effect caused by an electric field. Significantly larger values of $h(r)$, of up to several tens of mm, are obtained for ferrofluids, since these liquids have a much higher magnetic permeability. Therefore, observation and measurement of the Moses effect in ferrofluids can be easier.

6. Experiment and results

The Moses effect, which occurs in a ferrofluid around a long, rectilinear conductor with the current directed vertically, was chosen for the study. For such a case, the previously derived equation (12) applies. Using the conductor as a magnetic field source allows the field intensity H to be changed easily by varying the current I. The choice of ferrofluid is justified by the larger values of $h(r)$, as presented earlier (see Table I, and Sect. 4), and the unavailability of results of Moses effect studies in this type of liquid. In the experimental setup, a transparent vessel open from the top and made of polyester was used. A wire was passed vertically through a hole in the center of the bottom of the vessel, in which an electric current flowed. The wire had a diameter of 3 mm, a length of 40 cm, and was made of copper. The passage of wire through the bottom of the vessel was sealed from below with silicone, and ferrofluid was poured into the vessel. If the current was not flowing, the surface of the ferrofluid surrounding the wire was flat. The Moses effect appeared during the current flow.

The ferrofluid produced by Supermagnete and containing magnetite nanoparticles suspended in oil was used. The parameters of this ferrofluid were as follows: relative magnetic permeability $\mu_r = 2.14$, density $\rho = 1.59 \times 10^3$ kg/m^3, and surface tension coefficient $\alpha = 0.021$ N/m. The magnetic permeability was determined using a weighing magnetometer and was found to show no variation greater than $\pm 2\%$ in a magnetic field of 0–5 mT induction. During current flow, the ferrofluid level around the wire was raised by the Moses effect to a height of $h(r)$. The current intensity was varied in 10 A steps between 0 and 140 A. The current was switched on for a duration of 2 s, with an interval of at least 3 min between switches. During this time, the temperature of the wire and ferrofluid,

Fig. 5. Example of the shape of the free surface of the ferrofluid surrounded by a wire with radius $r = 1.5$ mm for current intensity $I = 140$ A. (Photo made by the author).

monitored using a Bosch GTC 400 C thermal imaging camera with a sensitivity of 50 mK, returned to the value from before the current was switched on.

The ferrofluid free surface around the wire was photographed using a Canon EOS R7 camera with a 35 Mpx sensor, giving a maximum resolution of 6960×4649 px. One of the ferrofluid surfaces captured this way is shown in Fig. 5. The resulting photographs were magnified 25 times, and the outline of the ferrofluid free surface was used to measure $h(r)$. Based on the results of these measurements, graphs of $h(r)$ and $h(I)$ were drawn on a linear scale, obtaining the relationships shown in Figs. 6 and 7. New independent variables r^{-2} and I^2 were then introduced and a logarithmic scale applied, both for the independent variables and for the dependent variables $h(r^{-2})$ and $h(I^2)$. The resulting graphs are shown in Figs. 8 and 9.

7. Discussion of results

Although the ferrofluid free surface image due to the Moses effect in ferrofluids is analogous to that in paramagnetic liquids, on the microscopic scale, this effect in ferrofluids occurs differently. Dia- or paramagnetic liquids are homogeneous on the molecular scale. An external magnetic field directly interacts with all the molecules of these liquids. The forces generated then give rise to a certain spatial distribution of pressure, which causes changes in the height of the liquid level. This manifests itself as a change in the shape of the free surface of the liquid, called the Moses effect. Ferrofluids on a microscopic scale have a heterogeneous structure. The external magnetic field interacts much more strongly with the nanoparticles suspended in it than with the surrounding dispersion liquid and surfactant molecules. The forces of this interaction cause changes in the position of the magnetic nanoparticles, which are transferred to the molecules of the dispersion liquid. This transfer is made possible by the viscosity forces of the

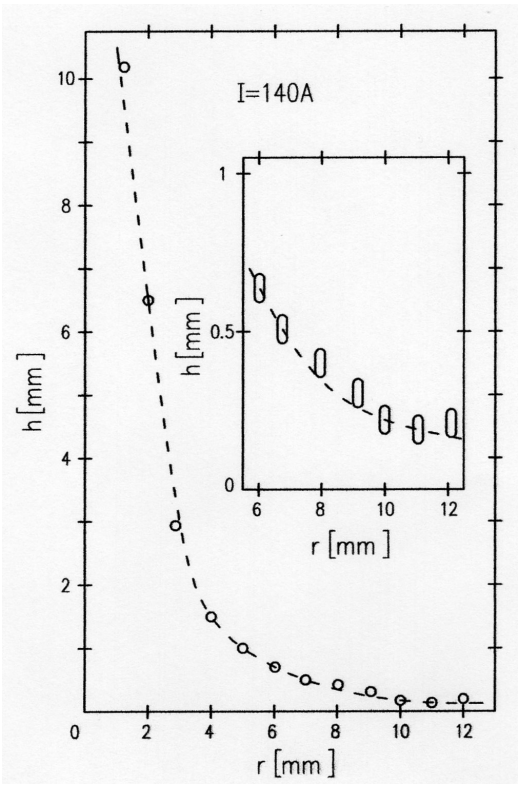

Fig. 6. Results of measurements of the ferrofluid level height h at distances r from the copper wire axis 2 for current intensity $I = 140$ A. The dashed line shows the results of calculations according to (12).

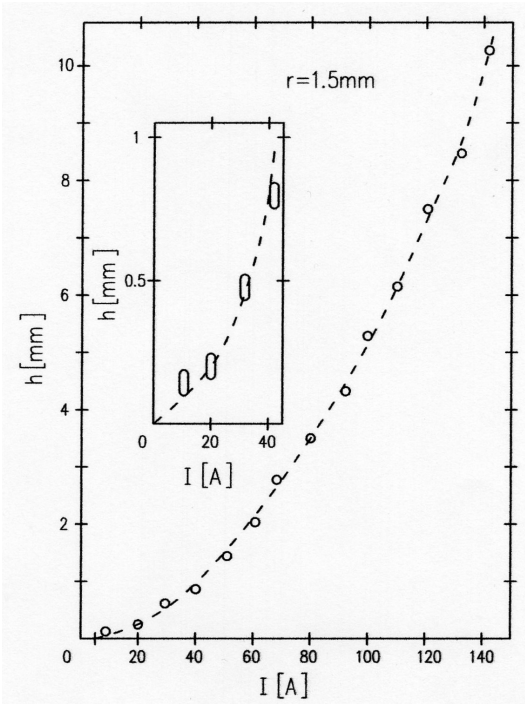

Fig. 7. Results of measurements of ferrofluid level height h on the surface of copper wire 2 with radius $r = 1.5$ mm for current intensity I. The dashed line shows the results of calculations according to (12).

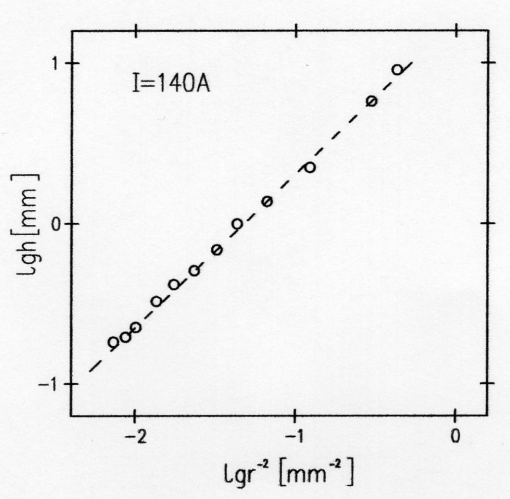

Fig. 8. Dependence of the height of the ferrofluid level h on r^{-2} on a logarithmic scale obtained from the data in Fig. 6. The dashed line shows the results of calculations according to (12).

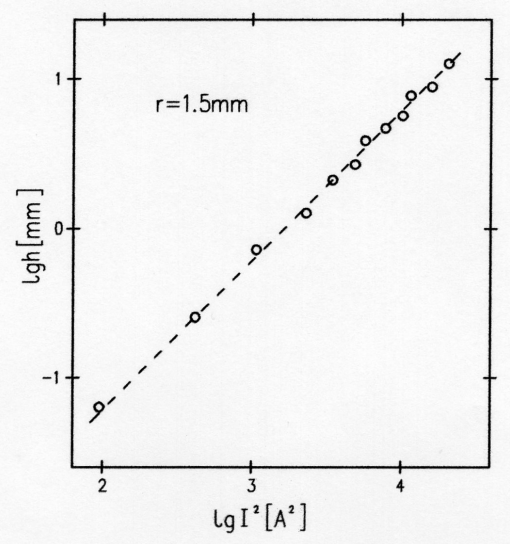

Fig. 9. Dependence of the height of the ferrofluid level h on I^2 on a logarithmic scale obtained from the data in Fig. 7. The dashed line shows the results of calculations according to (12).

dispersion liquid and the adhesion forces of the nanoparticles and the dispersion liquid. As a result, a spatial pressure distribution is generated throughout the volume of the ferrofluid, which produces a similar macroscopic effect as in the case of dia- or paramagnetic liquids. Thus, although in ferrofluids the transfer of magnetic interactions occurs indirectly, on a macroscopic scale, the final effect is similar to that in homogeneous liquids on a molecular scale. If the intensity of the magnetic field applied to the ferrofluid is sufficiently high, the nanoparticles begin to approach each other and form chains, which will then cluster into columns [45]. This is caused by the magnetization and rotation of the nanoparticles. Then their dissimilar poles attract each other and aim to align as close to each other as possible. On a macroscopic scale, this is observed to produce a characteristic needle-like structure on the free surface of the ferrofluid. This effect does not occur during the Moses effect of dia- and paramagnetic liquids, nor did it occur on the surface of the applied ferrofluid. Otherwise, the description of the Moses effect within the scope of the considerations adopted in this article would be impossible, as such an effect is not described by the derived formulae (12)–(15).

There is also an interesting conclusion from the derived formula (12), which is reached after introducing the relation between the current intensity I and its density j. For a wire with a circular cross-section, this relation is expressed by

$$I = \pi r^2 j. \tag{21}$$

After substituting the relation (21) into (12), one obtains

$$h(r) = \frac{\mu_0(\mu_r - 1)\, j^2 r^2}{8\rho g}. \tag{22}$$

The current density j must not be too high, as it is limited by the properties of the wire material. Too high a value of j causes, among other things, an excessive increase in the temperature of the wire and the ferrofluid in its surroundings. In this situation, for higher ferrofluid level heights $h(r)$, the wire radius r must be increased. This is exactly what was done in the experimental setup built, using a wire with a relatively large cross-sectional radius $r = 1.5$ mm. This allowed a maximum current of $I = 140$ A to flow through the wire without a noticeable increase in the temperature of the wire and the ferrofluid.

The surface tension of the ferrofluid α should be taken into account in the discussion of the uncertainty of the results. Since the free surface of the ferrofluid is concave, this surface tension causes an additional pressure directed vertically upwards. The value of this pressure was calculated from the Young–Laplace formula [46]. The previously reported values of the ferrofluid's parameters and the main radii of curvature of its free surface, determined from photographs, were used for the calculations. The additional pressure values obtained did not exceed 4.5% of the hydrostatic pressure of the ferrofluid due to the magnetic field. Since the pressure caused by the curvature of the surface is directed vertically upwards, this may contribute to the systematic error of overestimating the measured ferrofluid level heights $h(r)$.

It should also be recalled that (12) was derived for an infinitely long, current-carrying wire and a horizontal field gradient direction. In the constructed experimental system, the length of the wire in which the current flowed was 40 cm. In addition, the ferrofluid was also affected by the magnetic field generated by the other elements of the electrical circuit.

These elements influenced both the value of the horizontal component of the magnetic field intensity in the ferrofluid and the occurrence of the vertical component of this intensity. In addition, the ferrofluid was not shielded from the Earth's magnetic field, which also has a horizontal and vertical component. The values of each of these H_z components were assumed to be 78 A/m [3]. The detailed dimensions of the components of the experimental system, the given H_z and current values, were used to calculate the maximum change in magnetic field intensity in the volume occupied by the ferrofluid and caused by the described factors. A value of $\pm 4.5\%$ of the magnetic field intensity produced by an infinitely long current-carrying conductor was obtained without these factors present. Direct measurements were also made of the field intensity in the volume of the vessel, which showed that this variation did not exceed 3% of the field intensity produced by the infinitely long conductor. A TM-197 meter with a sensitivity of ± 0.01 mT with a Hall effect meter was used, allowing measurements with an uncertainty of not more than $\pm 1\%$. As stated earlier, the relative magnetic permeability of the ferrofluid μ_r showed no variation greater than $\pm 2\%$ in a magnetic field of 0–5 mT. An induction of 5 mT corresponds to a magnetic field intensity of 4×10^4 A/m. The maximum magnetic field intensity was produced at the surface of the wire by a current of $I = 140$ A and was 1.49×10^4 A/m. It was therefore assumed that the value of μ_r was constant during the measurements.

From the derived formula (12), it follows that this height is directly proportional to the square of the current I, flowing in the wire, and inversely proportional to the square of the distance from the axis of this wire r. Therefore, the theoretical curve in Fig. 6 is a parabola, while the theoretical curve in Fig. 7 is a hyperbola. After applying the new coordinates I^2 and r^{-2}, both curves are transformed into straight lines, shown in Figs. 8 and 9. Due to the large ranges of change in the values of the two dependent variables $h(I^2)$ and $h(r^{-2})$, it is advantageous to use a logarithmic scale to make these graphs, as this increases the resolution of the results for small values of these variables. Magnifying the photographs 25 times and using a ruler with a 0.5 mm scale allowed the ferrofluid level heights $h(r)$ to be measured with an uncertainty of less than ± 0.02 mm. Accordingly, all the results of the measurements of $h(r)$ shown in Figs. 6–9 are within this uncertainty. It should be noted, however, that the resulting relative uncertainty of the measurement results of $h(r)$ varies due to the large range of variability of these values. For larger values of $h(r)$ (e.g., $h(r) > 1$ mm) the relative uncertainty is very small and does not exceed 2%, while for the smallest values of $h(r)$ (e.g., $h(r) = 0.05$ mm for $I = 10$ A — see Fig. 7, or $h(r) = 0.35$ mm for $r = 12$ mm — see Fig. 6) the relative uncertainties are large and amount to 40% and 6%, respectively.

8. Conclusions

Taking into account all the previously discussed uncertainties, it can be concluded that the total uncertainty of agreement between the measured values of $h(r)$ and the results of the calculation based on formula (12) does not exceed 10% except for a few of the smallest values of $h(r)$. The uncertainty of these results can be reduced by an easy improvement of the method used, which consists in taking photographs of the free surface of the ferrofluid with a higher resolution. Such photographs will allow an increase in their magnification without the appearance of a pixel structure that causes uncertainty in the measurements.

An important advantage of using ferrofluid to study the Moses effect proved to be the obtaining of large level heights of this liquid, $h(r)$. The values of $h(r)$ near the wire were more than 10 mm larger than at the walls of the vessel. The obtained heights $h(r)$ are also ca. 10^4–10^5 times greater than in dia- or paramagnetic liquids placed in a magnetic field of the same intensity. The large heights $h(r)$ justify the use of the name "giant Moses effect" for this case. Thanks to the large values of $h(r)$, special instruments, such as interferometers, necessary when studying the Moses effect in dia- or paramagnetic liquids, do not have to be used to perform the measurements [6, 7, 44]. Furthermore, the construction of the experimental setup is cheaper, and the measurements can be performed more easily. Obtaining large heights of ferrofluid level $h(r)$ provides opportunities for practical applications of the Moses effect in these liquids, e.g., to determine their permeability, magnetization curve, or field intensity.

Finally, the Moses effect is also of great educational importance. This effect makes it possible to perform demonstrations, showing the behavior of liquids in different force fields. An introduction to the description of this effect for educational purposes can be found in Wikipedia [47]. Among the demonstrations, the following are worth mentioning:

(i) The deviation from vertical of a thin stream of water due to attraction to an electrified body.

(ii) The sliding of a razor blade lying on the surface of water from its elevation ("hill"), which is created by attraction to an electrified body.

(iii) Deviation from vertical of the path of air bubbles, rising in the water due to interaction with a magnet [15, 20].

(iv) Changing the shape of water droplets, flowing down a trough of paraffin to a more spherical shape as a result of their electrification by friction during this movement.

(v) The change in the shape of the surface of ferrifluids and electrofluids when a magnet, or an electrified body, is brought close [21]. Such experiments can be shown both in a general

TABLE II

Formulas for the height of the liquid level $h(r)$ in fields with axial symmetry produced by selected sources. Meaning of the symbols: I — current, λ — linear density of charge, q — point charge, r — distance from axis or center, l — length of wire, p_m and p_e — magnetic and electric moment, respectively, μ_0 and ε_0 — vacuum magnetic and electric permeability, respectively, μ_r and ε_r — relative permeabilities of liquid magnetic and electric, respectively, g — acceleration of Earth's gravity, ρ — density of liquid.

Source of field	Field		Conditions
	magnetic	electric	
long straight-line wire	$h(r) = \frac{\mu_0(\mu_r-1)I^2}{8\pi^2\rho g r^2}$	$h(r) = \frac{(\varepsilon_r-1)\lambda^2}{8\pi^2\varepsilon_0\rho g r^2}$	in a distance r from the axis
section of straight-line wire	$h(r) = \frac{\mu_0(\mu_r-1)I^2}{8\pi^2\rho g r^2}\left[\frac{l^2}{\sqrt{4r^2+l^2}}\right]$	$h(r) = \frac{(\varepsilon_r-1)\lambda^2}{8\pi^2\varepsilon_0\rho g r^2}\left[\frac{l^2}{\sqrt{4r^2+l^2}}\right]$	at the symmetrical in a distance r from the axis
dipol	$h(r) = \frac{\mu_0(\mu_r-1)p_m^2}{32\pi^2\rho g r^6}$	$h(r) = \frac{(\varepsilon_r-1)p_e^2}{32\pi^2\varepsilon_0\rho g r^6}$	at the axis in a distance r from the center, $r \gg$ than the length of p_m, p_e
	$h(r) = \frac{\mu_0(\mu_r-1)p_m^2}{16\pi^2\rho g r^6}$	$h(r) = \frac{(\varepsilon_r-1)p_e^2}{16\pi^2\varepsilon_0\rho g r^6}$	at the symmetrical in a distance r from the axis, $r \gg$ than the length of p_m, p_e
point or spherical charge		$h(r) = \frac{(\varepsilon_r-1)q^2}{32\pi^2\varepsilon_0\rho g r^4}$	in a distance r from the center of the charge

physics course and in more advanced lectures, such as fluid mechanics. The undoubted advantages of the aforementioned experiments are that they are spectacular and easy to perform.

Appendix: Formulas for other fields with cylindrical symmetry

The assumption that the field gradient has only one horizontal component, directed along r, is fulfilled in special cases of spatial field distributions that have cylindrical or spherical symmetry. For further analysis, examples of the most common sources with the properties mentioned above were selected, and the formulas for the field intensity generated by these sources, known from electrodynamics, were used [25]. The field intensity formulas were substituted into (9), and (10), and the formulas for the height of the liquid level $h(r)$ in the Moses effect caused by these sources were derived. The obtained results are given in Table II.

Formulas contained in Table II can also be applied in a limited area for horizontally directed field sources, e.g., for an infinitely long current-carrying conductor directed horizontally and a liquid located under, or above, this conductor. In these cases, the assumptions used to derive the discussed formulae are satisfied at points lying on vertical lines and passing through the axis or center of these sources. Then, $h(r)$ is a good result for the height of the liquid level at these points.

References

[1] N. Hirota, T. Homma, H. Sugawara et al., *Jpn. J. Appl. Phys.* **34**, L991 (1995).

[2] K. Kitazawa, Y. Ikezoe, H. Uetake, N. Hirota, *Phys. B Condens. Mater.* **294–295**, 709 (2001).

[3] W.M. Haynes, *CRC Handbook of Chemistry and Physics, A Ready-Reference Book of Chemical and Physical Data*, Taylor and Francis Group, Boca Raton 2014, p. 12-108.

[4] D. Shulman, Ph.D. Thesis, Ariel University 2023.

[5] D. Shulman, *J. Magn.* **28**, 64 (2023).

[6] D. Shulman, *Rev. Sci. Instrum.* **94**, 045114 (2023).

[7] D. Shulman, *J. Appl. Phys.* **133**, 173905 (2023).

[8] D. Shulman, M. Lewkowicz, E. Bromashenko, *J. Macromol. Sci. B* **61**, 1463 (2022).

[9] D. Shulman, M. Lewkowicz, E. Bromashenko, *J. Magn. Magn. Mater.* **571**, 170553 (2023).

[10] T. Lemura, T. Kimura, M. Sugitani, M. Kumakura, *Adv. Mater.* **18**, 1549 (2006).

[11] H. Sugawara, N. Hirota, T. Homma et al., *J. Appl. Phys.* **79**, 4721 (1996).

[12] P.G. Meyer, V. Adlakha, H. Kantz, K.E. Bassler, *New J. Phys.* **20**, 113033 (2018).

[13] S. Ueno, M. Iwasaka, *J. Appl. Phys.* **75**, 7177 (1994).

[14] M. Frenkel, V. Danchuk, V. Multanen, I. Legchenkova, Y. Bormashenko, O. Gendelman, E. Bormashenko, *Langmuir* **34**, 6388 (2018).

[15] Z. Chen, J. Ellis, E.D. Dahlberg, *Rev. Sci. Instum.* **83**, 095112 (2012).

[16] T. Kimura, M. Yamato, A. Nara, *Langmuir* **20**, 572 (2004).

[17] E. Bromashenko, *Adv. Colloid Interface Sci.* **269**, 1 (2019).

[18] N. Derby, S. Olbert, *Am. J. Phys.* **78**, 229 (2010).

[19] V. Labinac, D. Kotnik-Karuza, *Am. J. Phys.* **74**, 621 (2006).

[20] D. Laumann, *Phys. Teach.* **56**, 352 (2018).

[21] Z. Chen, E.D. Dahlberg, *Phys. Teach.* **49**, 144 (2011).

[22] L.D. Landau, J.S. Bell, M.J. Kearesley, L.P. Pitajewski, F.M. Lifchitz, J.B. Sykes, *Electrodynamics of Continuous Media*, Elsevier Butterworth Heinmann, Oxford 1984.

[23] Y.T. Tomoda, J. Segawa, T. Takamura, *J. Phys. Earth* **20**, 267 (1972).

[24] A. Łyszkowicz, *J. Planet. Geod.* **35**, 31 (2000).

[25] M.A. Plouns, *Applied Electrodynamics*, McGraw-Hill, New York 1978.

[26] W.E. Willshaw, L. Rushforth, A.G. Stainsby, R. Latam, A.W. Balls, A.H. King, *J. Institut. Electr. Eng.* **93**, 985 (2018).

[27] L. Zheoyang, L. Yuxin, L. Ruxin, *Laser Photon. Rev.* **17**, 2100705 (2023).

[28] E.W. Gaul, *Appl. Opt.* **49**, 1676 (2010).

[29] W.M. Winslow, *J. Appl. Phys.* **20**, 1137 (1949).

[30] J.E. Stangroom, *Phys. Technol.* **14**, 290 (1983).

[31] W. Wen, X. Huang, S. Yang, K. Lu, P. Sheng, *Natur. Mater.* **2**, 727 (2003).

[32] R. Hades, G. Warr, G. Gregory, R. Atkin, *Chem. Rev.* **115**, 6357 (2015).

[33] C. Scherer, A.M. Figueiredo Neto, *Brazil. J. Phys.* **35**, 718 (2005).

[34] R.E. Rosensweig, *Sci. Am.* **247**, 136 (1982).

[35] M. Shliomis, *Phys. Rev.* **64**, 060501(R) (2001).

[36] A.Y. Solovyova, E.A. Elfimova, *J. Magn. Magn. Mater.* **495**, 165846 (2020).

[37] C. Gollwitzer, M. Krekhova, G. Lattermann, I. Rehberg, R. Richter, *Soft Matter* **5**, 2093 (2009).

[38] S. Bednarek, *J. Magn. Magn. Mater.* **323**, 957 (2011).

[39] C.S.S.R. Kumar, F. Mohammad, *Adv. Drug Deliv. Rev.* **63**, 789 (2011).

[40] A. Bibo, R. Masana, A. King, G. Li, M.F. Daqaq, *Phys. Lett. A* **376**, 2163 (2012).

[41] L. Melillo, K. Raj, *J. Audio Eng. Soc.* **29**, 132 (1981).

[42] J. Philip, T. Jaykumar, P. Kalyanasundaram, B. Raj, *Meas. Sci. Technol.* **14**, 1289 (2003).

[43] I. Legchenkova, G. Chaniel, M. Frenkiel, Y. Bormashenko, S. Shoval, E. Bormashenko, *Surf. Innov.* **6**, 231 (2018).

[44] J. Dong, R. Miao, J. Qi, *J. Appl. Phys.* **100**, 124914 (2006).

[45] E. Blums, A. Cebers, M.M. Maiorov, *Magnetic Fluids*, Walter de Gruyter, Berlin 1997.

[46] F. Brochard-Wyart, D. Quéré, *Capillarity and Wetting Phenomena — Drops, Bubbles, Pearls, Waves*, Ed. A. Reisinger, Springer, Berlin 2002.

[47] Moses effect, Wikipedia (access 07.2025).